DEM GENERATION USING ERS-1/2 INTERFEROMETRIC SAR DATA

Shi Shiping
Xian Research Institude of Surveying and Mapping
No.1 Mid-Yanta Road , Xi'an 710054 China

Working Group IV/2

KEY WORDS：Interferometry, SAR, Image matching, Phase unwrapping, DEM.

ABSTRACT

Accurate digital elevation model(DEM) can be producted by using interferometric SAR data. We have developed a new software on PC's that can automatically generate DEM from single look complex SAR pairs. The least-squares image matching method based on SAR multi-look intensity images has been used to register complex image pair. The typical accuracy of 0.02-0.04 pixel size can be obtained on multi-look SAR images. We also present a new set of equations for calculating three dimensional coordinates at each pixel from unwrapped phases. The orbital position, attitude and baseline as well as phase constant have been involved in the equations. Using at least six ground control points, it is possible to refine interferometric baseline, and estimate the phase constant, the orbit and attitude parameters simultaneously. Test results are provided for ERS-1/2 interferometric SAR scene pair acquired over Etna area in Italy.

1 INTRODUCTION

Synthetic aperture radar(SAR) interferometry is a powerful technique for the generation of accurate digital elevation model(DEM)(Zebker and Goldstein,1986)，the detection of surface deformation(Massonnet et al.,1993),and calculation of the ice sheet motion(Goldstein et al.,1993). There are two ways to implement across-track interferometry. In the first approach, the two physical antennas displaced in across-track are mounted on a single platform.One antenna is used for transmitting and receiving radar signals,and the other for receiving only. These systems usually are used in airborne system and Shuttle Radar Topography Mission(SRTM). Second, interferometry was realized by utilizing a single antenna on the platform in a nearly exact-repeating orbit. Repeat-track interferometry has significant advantage in low cost and simplity because it uses a single antenna. For repeat-track interferometry two SAR images were acquired at different time, the imaged surface may change during the observation to introduce correlation decrease. This is usually called temporal decorrelation. The low correlations between the signals result in large interferometric phase error and height estimate error. With the ERS-2 satellite was launched, ERS-1/2 repeat-tract time interval is 24-houses, the performance of topographic mapping for ERS-1/2 interferometric SAR will be improved. In certain conditions, DEM generated by ERS-1/2 SAR can fulfil the heigh accuracy of 1:50000 map.

2 INTERFEROMETRIC SAR DATA PROCESSING

2.1 Image Registration and Interferogram Production

In order to form the interferogram, the single look complex(SLC) image pair has to be co-registered. We present a new registration method. This approach is a multi-lever matching technique based on the SAR intensity images. First, we select one of image pair as a geometric reference, and will be called the master image. The other will be called the slave image. Two pixels located at the same range in the master image do not share the same range in the slave image if the elevation of the points they represent on the ground differ. We define a regular grid of anchor points in the master image. We find correspondent point in slave intensity SAR image using the standard local correlation technique. The offsets of matching point are obtained. This made matching point to a pixel accuracy. Then we started second-lever matching---least squares image matching. The least squares matching (LSM) is based on the principle which minimizes the sum of the squares for gray value difference.

The linear observation equation for LSM is expressed as：

$$\Delta g(z_i) + v(z_i) = \sum (\frac{\partial S''}{\partial a_m})_0 \cdot da_m + \sum (\frac{\partial S''}{\partial h_k})_0 \cdot dh_k \qquad (m=1,6;k=0,1) \qquad (1)$$

where $\Delta g(z_i)$ is gray difference for correspondent pixels in the two matching windows; $v(z_i)$ is observation error; S'' is slave intensity image transformed by geometric and radiant transformation (transformation parameters are a_m and h_k ,respectively) . da_m and dh_k are corrections for unknown transformation parameters.

Each correspondent pixel pair in matching windows may give an observation equation. The corrections da_m and dh_k for unknown transformation parameters can be solved using the least squares solution. The transformation parameters were calculated by expressions:

$$a_m^{(i)} = a_m^{(i-1)} + da_m \qquad h_k^{(i)} = h_k^{(i-1)} + dh_k$$

The weights of the observations are set to be 1.The solution was performed by iteration.

Due to speckle noise effect for SAR image, it is adverse to use least squares in single look complex SAR pair. So,we first generate multi-look SAR intensity images, and perform matching for multi-look image pair. The offsets for this image pair are derived, and results are then rescled to account for the integer factor of reduction between multi-look images and single look complex images. The registration and resampling are performed in SLC images.

The registration of any pixel can be performed after the offsets of grid points were formed. For any point in master image, pixel offsets of correspondent point in slave image were calculated by using bilinear interpolation as follows.

$$\left.\begin{aligned} x' &= a_0 + a_1 x + a_2 y + a_3 xy \\ y' &= b_0 + b_1 x + b_2 y + b_3 xy \end{aligned}\right\} \qquad (2)$$

where x' and y' are offsets for slave image. The x and y are coordinates for this point. The $a_0 \cdots b_3$ are transformation parameters.

The next processing step is the resampling for slave complex image. We use the bilinear interpolation to perform this task. The resampled value of any point P is:

$$P = a + bi = (1-\Delta x)(1-\Delta y)P_{11} + (1-\Delta x)\Delta y P_{12} + \Delta x(1-\Delta y)P_{21} + \Delta x \Delta y P_{22} \qquad (3)$$

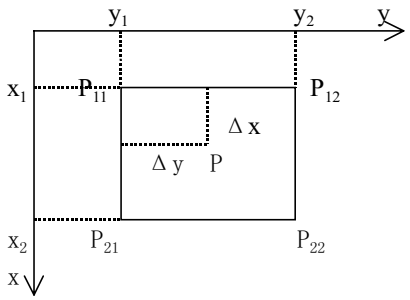

Figure 1 Bilinear interpolation

where $P_{11}, P_{12}, P_{21}, P_{22}$ are complex pixel values.

It is possible to form an interferogram after all pixels were registered. We assume that M_{ij} is the complex pixel value in the master image, S_{ij} is equivalent in the co-registered complex slave image, and T_{ij} is complex pixel in the interferogram, we have:

$$T_{ij} = M_{ij} \cdot S_{ij}^* \qquad i = 1, \cdots, n, \quad j = 1, \cdots, m$$

where S_{ij}^* is the complex conjugate of pixel S_{ij}.

2.2 Coherence Calculation

For the co-registered image pair, the coherence was computed as follows：

$$\rho = \left| \frac{1}{N_1 N_2} \sum_{\substack{i=1,N1 \\ j=1,N2}} M_{ij} \cdot S_{ij}^{*} \right| \Bigg/ \left(\sqrt{\frac{1}{N_1 N_2} \sum_{\substack{i=1,N1 \\ j=1,N2}} M_{ij} \cdot M_{ij}^{*}} \cdot \sqrt{\frac{1}{N_1 N_2} \sum_{\substack{i=1,N1 \\ j=1,N2}} S_{ij} \cdot S_{ij}^{*}} \right) \tag{4}$$

where M_{ij} is the complex conjugate of pixel M_{ij}; N_1 N_2 are number of pixels in azimuth and in slant range, respectively.

2.3 Flat Earth Phase Removal

In order to reduce the phase noise and simplify the phase unwrapping procedure, flat earth phase removal was carried out. A tangent plane to the scene center or spherical surface can be used as the reference surface for flat earth phase removal. To further reduce interferometric phase noise in mountainous areas, a coarse digital elevation model could replace the plane or spherical surface as the reference. We used the tangent plane of the scene center as flat earth phase removal reference. The planar phase to be subtracted is calculated as follows:

$$\phi_{ij} = \frac{4\pi}{\lambda_C} B \cos\beta \qquad , \beta = \alpha + \sin^{-1} \frac{H}{r_{ij}} \qquad i = 1, \cdots, n, \quad j = 1, \cdots, m \tag{5}$$

where λ_C is wavelength, B is baseline distance, β is angle between the baseline and line of look, α is the baseline angle with respect to horizontal, H is orbital altitude, r_{ij} is the range to a point on the ground. B and α can be calculated from the satellite orbital data.(see section 3.1)

Removal of the phase term φ_{ij} from each pixel produces the flatted interferogram, ready for input to the phase unwrapped step.

2.4 Adaptive Filter and Phase Unwrapping

In order to reduce the phase noise and to facilitate the phase unwrapping, the raw interferogram was filtered using a multi-look technique, typically 2 in range and 10 in azimuth. The filtered flattened interferogram was then unwrapped using least squares phase unwrapping method.

The interferometric phases are measured mode 2π, that is,the integral number of phase cycles on each measurement is lost. To reconstruct digital elevation model, the integral number of phase cycles lost have to be recovered. This procedure is known as phase unwrapping. When there are no noise or aliasing effect in the measurement phases, phase unwrapping is very simple and straightforward. A simple integration procedure,in which the partial derivatives of the phase data are extracted and then integrated along vertical or horizontal lines suffices to produce the unwrapped phase. In practice, however, there are noise and aliasing effects that cause inconsistencies in the phase. The simple integration procedure can not be applied in this case, because it propagates and accumulates these phase inconsistencies,giving rise to very large error in the result.

Two main phase unwrapping methods in common use today are residue-cut phase unwrapping (Goldstein et al.,1988) and least squares methods(Ghiglia and Romero,1994).We selected least squares procedure to perform phase unwrapping. Least squares phase unwrapping is based on the principle that determines a smooth unwrapped phase function that minimizes the difference between the gradients calculated from the wrapped phase and the presumed smooth unwrapped phase. Assuming φ_{ij} denotes the wrapped phase of any pixel in image, ϕ_{ij} and is correspondent unwrapped phase. Phase observation equation is expressed as：

$$V = A\phi - L \tag{6}$$

where V is the residual vector, A is coefficient matrix, ϕ is unknown unwrapped phase, L is observiation related to φ_{ij}.

The least squares solution is obtained as：

$$\phi = \left(A^T A\right)^{-1} A^T L \tag{7}$$

When certain phase values are known to be corrupted due to noise, aliasing or other degradation, the weighted least squares method should be used to reduce the poor effect for unwrapping. Assuming equation (6) has a weight matrix P, The least squares solution is ：

$$\phi = \left(A^T PA\right)^{-1} A^T P L \tag{8}$$

We used conjugate gradient method to solve equation (8) iteratively. The accuracy of the solution depend on the choice of weight to apply to each point of the measured phase. The coherence of interferogram provides the quality information of measured phase, we used coherence map to construct the weight map of the observation phases.

3 CALCULATION OF THREE DIMENSIONAL COORDINATES FOR TARGET POINT

3.1 Estimating the Baseline Vector Using Orbital Data

In order to simplify baseline estimation, we establish an assistant coordinate system, whose origin is in the master orbit

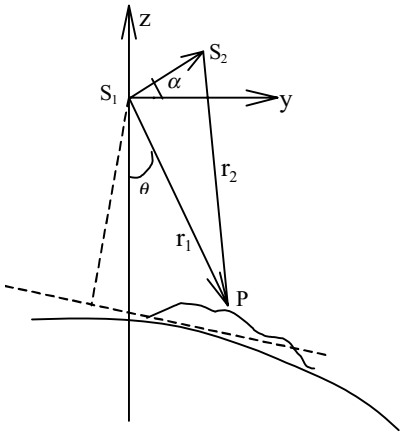

Figure 2 Geometry of interferometric SAR

position relative to the mid-scene, z-axis is in ray linking this point and center of earth, x-axis is in the orbital pane and perpendiculur to the z-axis and towards the direction of satellite motion, and y-axis completes a right hand coordinate system. The interferometric baseline is defined as the distance vector between two orbit positions corresponding to the time when the satellite imaged the same target on the earth's surface. The three coordinate components of slave orbit position were expressed as time dependent polynomial. The polynomial coefficients are estimated by the orbital node data, and the slave orbital position of any time can be calculated by this polynomial. The baseline vector can be calculated when the x component of slave orbital position is zero. The expressions are：

$$\left.\begin{aligned} B &= \sqrt{y^2 + z^2} \\ \alpha &= tg^{-1}\frac{z}{y} \end{aligned}\right\} \tag{9}$$

3.2 Refining The Baseline,Orbital and Attitude Parameters

Topographic mapping equation for interferometric SAR can be written as (Shi,1996):

$$\vec{r}_{target} = \vec{r}_{radar} + \vec{n}_{los} \cdot r \tag{10}$$

where r is the slant range, $\vec{n}_{los}$ is an unit vector in the line of sight direction. Rewritten as matrix form：

$$\begin{bmatrix} X \\ Y \\ Z \end{bmatrix} = \lambda \begin{bmatrix} a_1 & a_2 & a_3 \\ b_1 & b_2 & b_3 \\ c_1 & c_2 & c_3 \end{bmatrix} \begin{bmatrix} 0 \\ r\sin\theta \\ -r\cos\theta \end{bmatrix} + \begin{bmatrix} X_S \\ Y_S \\ Z_S \end{bmatrix} \tag{11}$$

$$\theta = \frac{\pi}{2} - \arccos\left(\frac{\lambda_C}{4\pi B}\phi\right) + \alpha$$

where X, Y, Z are ground coordinates of any point; $a_1, a_2, \cdots, c_3$ are elements of the rotation matrix expressed as function of three attitude angles φ, ω, κ; λ is scale factor. θ is false look angle;. X_s, Y_s, Z_s are satellite position; ϕ is interferometric absolute phase.

$$\begin{aligned}
a_1 &= \cos\varphi\cos\kappa - \sin\varphi\sin\omega\sin\kappa \\
b_1 &= \cos\omega\sin\kappa \\
c_1 &= \sin\varphi\cos\kappa + \cos\varphi\sin\omega\sin\kappa \\
a_2 &= -\cos\varphi\sin\kappa - \sin\varphi\sin\omega\cos\kappa \\
b_2 &= \cos\omega\cos\kappa \\
c_2 &= -\sin\varphi\sin\kappa + \cos\varphi\sin\omega\cos\kappa \\
a_3 &= -\sin\varphi\cos\omega \\
b_3 &= -\sin\omega \\
c_3 &= \cos\varphi\cos\omega
\end{aligned}$$

The orbital position, attitude parameters and baseline distance can be characterized by linear or low order polynomial function. Here are expressed as linear functions.

$$\begin{aligned}
X_S &= X_{S0} + \dot{X}_S(t - t0) \\
&\vdots \\
B &= B_0 + \dot{B}(t - t0)
\end{aligned}$$

Linearizing equation(11)，we obtain the observation equation：

$$V_1 = A_1 X - L_1 \qquad P_1 \tag{12}$$

where,

$$\begin{aligned}
V_1 &= \begin{bmatrix} V_X & V_Y & V_Z \end{bmatrix}^T \\
A_1 &= \begin{bmatrix} a_{11} & a_{12} & \cdots & a_{117} \\ a_{21} & a_{22} & \cdots & a_{217} \\ a_{31} & a_{32} & \cdots & a_{317} \end{bmatrix} \\
X &= \begin{bmatrix} \Delta X_{s0} \Delta Y_{s0} \Delta Z_{s0} \Delta\varphi_0 \Delta\omega_0 \Delta\kappa_0 \Delta\lambda_0 \Delta\dot{X}_s \Delta\dot{Y}_s \Delta\dot{Z}_s \Delta\dot{\varphi} \Delta\dot{\omega} \Delta\dot{\kappa} & \Delta\dot{\lambda} \Delta B_0 \Delta\dot{B} \Delta\phi_C \end{bmatrix}^T \\
L_1 &= \begin{bmatrix} L_X & L_Y & L_Z \end{bmatrix}^T
\end{aligned}$$

where $\Delta X_{s0}, \Delta Y_{s0}, \Delta Z_{s0}$ *and* $\Delta\varphi_0$, $\Delta\omega_0$, $\Delta\kappa_0$ denote corrections for orbital position and attitude at time t0,respectively; $\Delta\dot{X}_S, \Delta\dot{Y}_S, \Delta\dot{Z}_S$ *and* $\Delta\dot{\varphi}$, $\Delta\dot{\omega}$, $\Delta\dot{\kappa}$ denote corrections for correspondent rate, respectively; $\Delta\lambda_0$ *and* ΔB_0 denote corrections of the scale and baseline length at time t0, respectively; $\Delta\lambda$ *and* ΔB denote corrections for correspondent rate, respectively; $\Delta\phi_C$ is correction for phase constant; P_1 indicates the weight matrix.

$$\begin{aligned}
a_{11} &= \frac{\partial X}{\partial X_{s0}} = 1, a_{12} = \frac{\partial X}{\partial Y_{s0}} = 0, a_{13} = \frac{\partial X}{\partial Z_{s0}} = 0, a_{14} = \frac{\partial X}{\partial \varphi_0} = -\lambda(c_2 r\sin\theta - c_3 r\cos\theta) \\
a_{15} &= \frac{\partial X}{\partial \omega_0} = -\lambda(b_2 r\sin\theta - b_3 r\cos\theta)\sin\varphi \\
a_{16} &= \frac{\partial X}{\partial \kappa_0} = -\lambda(b_2 r\sin\theta - b_3 r\cos\theta)\cos\varphi\cos\omega - \lambda(c_2 r\sin\theta - c_3 r\cos\theta)\sin\omega \\
a_{17} &= \frac{\partial X}{\partial \lambda_0} = a_2 r\sin\theta - a_3 r\cos\theta
\end{aligned}$$

$$a_{18}=\frac{\partial X}{\partial \dot{X}_s}=t-t0\,,\ a_{19}=\frac{\partial X}{\partial \dot{Y}_s}=0\,,\ a_{110}=\frac{\partial X}{\partial \dot{Z}_s}=0$$

$$a_{111}=\frac{\partial X}{\partial \dot{\varphi}}=a_{14}(t-t0)\,,\ a_{112}=\frac{\partial X}{\partial \dot{\omega}}=a_{15}(t-t0)\,,\ a_{113}=\frac{\partial X}{\partial \dot{\kappa}}=a_{16}(t-t0)$$

$$a_{114}=\frac{\partial X}{\partial \dot{\lambda}}=a_{17}(t-t0)\,,\ a_{115}=\frac{\partial X}{\partial B_0}=\lambda\left(a_2 r+a_3 rtg\theta\right)\frac{\lambda_C\phi}{4\pi\left(B_0+\dot{B}\left(t-t_0\right)\right)^2}$$

$$a_{116}=\frac{\partial X}{\partial \dot{B}}=a_{115}\cdot\left(t-t_0\right)$$

$$a_{117}=\frac{\partial X}{\partial \phi_C}=\lambda\left(a_2 r+a_3 rtg\theta\right)\cdot\left(\frac{1}{B_0+\dot{B}(t-t0)}+\frac{\lambda_C\phi}{4\pi r(B_0+\dot{B}(t-t0))}\right)$$

$$a_{21}=\frac{\partial Y}{\partial X_{s0}}=0\,,\ a_{22}=\frac{\partial Y}{\partial Y_{s0}}=1\,,\ a_{23}=\frac{\partial Y}{\partial Z_{s0}}=0\,,\ a_{24}=\frac{\partial Y}{\partial \varphi_0}=0$$

$$a_{25}=\frac{\partial Y}{\partial \omega_0}=\lambda(a_2 r\sin\theta-a_3 r\cos\theta)\sin\varphi-\lambda(c_2 r\sin\theta-c_3 r\cos\theta)\cos\varphi$$

$$a_{26}=\frac{\partial Y}{\partial \kappa_0}=\lambda(a_2 r\sin\theta-a_3 r\cos\theta)\cos\varphi\cos\omega+\lambda(c_2 r\sin\theta-c_3 r\cos\theta)\sin\varphi\cos\omega$$

$$a_{27}=\frac{\partial Y}{\partial \lambda_0}=b_2 r\sin\theta-b_3 r\cos\theta$$

$$a_{28}=\frac{\partial Y}{\partial \dot{X}_s}=0\,,\ a_{29}=\frac{\partial Y}{\partial \dot{Y}_s}=t-t0\,,\ a_{210}=\frac{\partial Y}{\partial \dot{Z}_s}=0$$

$$a_{211}=\frac{\partial Y}{\partial \dot{\varphi}}=0\,,\ a_{212}=\frac{\partial Y}{\partial \dot{\omega}}=a_{25}(t-t0)\,,\ a_{213}=\frac{\partial Y}{\partial \dot{\kappa}}=a_{26}(t-t0)$$

$$a_{214}=\frac{\partial Y}{\partial \dot{\lambda}}=a_{27}(t-t0)\,,\ a_{215}=\frac{\partial Y}{\partial B_0}=\lambda\left(b_2 r+b_3 rtg\theta\right)\frac{\lambda_C\phi}{4\pi\left(B_0+\dot{B}\left(t-t_0\right)\right)^2}$$

$$a_{216}=\frac{\partial Y}{\partial \dot{B}}=a_{215}\cdot\left(t-t_0\right)$$

$$a_{217}=\frac{\partial Y}{\partial \phi_C}=\lambda\left(b_2 r+b_3 rtg\theta\right)\cdot\left(\frac{1}{B_0+\dot{B}(t-t0)}+\frac{\lambda_C\phi}{4\pi r(B_0+\dot{B}(t-t0))}\right)$$

$$a_{31}=\frac{\partial Z}{\partial X_{s0}}=0\,,\ a_{32}=\frac{\partial Z}{\partial Y_{s0}}=0\,,\ a_{33}=\frac{\partial Z}{\partial Z_{s0}}=1\,,\ a_{34}=\frac{\partial Z}{\partial \varphi_0}=\lambda(a_2 r\sin\theta-a_3 r\cos\theta)$$

$$a_{35}=\frac{\partial Z}{\partial \omega_0}=\lambda(b_2 r\sin\theta-b_3 r\cos\theta)\cos\varphi$$

$$a_{36}=\frac{\partial Z}{\partial \kappa_0}=\lambda(a_2 r\sin\theta-a_3 r\cos\theta)\cos\omega-\lambda(b_2 r\sin\theta-b_3 r\cos\theta)\sin\varphi\cos\omega$$

$$a_{37}=\frac{\partial Z}{\partial \lambda_0}=c_2 r\sin\theta-c_3 r\cos\theta$$

$$a_{38}=\frac{\partial Z}{\partial \dot{X}_s}=0\,,\ a_{39}=\frac{\partial Z}{\partial \dot{Y}_s}=0\,,\ a_{310}=\frac{\partial Z}{\partial \dot{Z}_s}=t-t0$$

$$a_{311}=\frac{\partial Z}{\partial \dot{\varphi}}=a_{34}(t-t0)\,,\ a_{312}=\frac{\partial Z}{\partial \dot{\omega}}=a_{35}(t-t0)\,,\ a_{313}=\frac{\partial Z}{\partial \dot{\kappa}}=a_{36}(t-t0)$$

$$a_{314}=\frac{\partial Z}{\partial \dot{\lambda}}=a_{37}(t-t0)\,,\ a_{315}=\frac{\partial Z}{\partial B_0}=\lambda\left(c_2 r+c_3 rtg\theta\right)\frac{\lambda_C\phi}{4\pi\left(B_0+\dot{B}\left(t-t_0\right)\right)^2}$$

$$a_{316}=\frac{\partial Z}{\partial \dot{B}}=a_{315}\cdot\left(t-t_0\right)$$

$$a_{317}=\frac{\partial Z}{\partial \phi_C}=\lambda\left(c_2 r+c_3 rtg\theta\right)\cdot\left(\frac{1}{B_0+\dot{B}(t-t0)}+\frac{\lambda_C\phi}{4\pi r(B_0+\dot{B}(t-t0))}\right)$$

$$L_x=X-(X_{s0}+\dot{X}_s(t-t0))-\lambda(a_2 r\sin\theta-a_3 r\cos\theta)$$

$$L_y = Y - (Y_{s0} + \dot{Y}_s(t - t0)) - \lambda(b_2 r \sin\theta - b_3 r \cos\theta)$$
$$L_z = Z - (Z_{s0} + \dot{Z}_s(t - t0)) - \lambda(c_2 r \sin\theta - c_3 r \cos\theta)$$

We can also give the following observation equation when the accurate enough satellite orbital data are known：

$$V_2 = A_2 X - L_2 \qquad P_2 \tag{13}$$

where

$$V_2 = \begin{bmatrix} V_{X_S} & V_{Y_S} & V_{Z_S} \end{bmatrix}^T$$
$$A_2 = \begin{bmatrix} 1 & 0 & 0 & 0 & 0 & 0 & 0 & 1 & 0 & 0 \cdots & 0 \\ 0 & 1 & 0 & 0 & 0 & 0 & 0 & 0 & 1 & 0 \cdots & 0 \\ 0 & 0 & 1 & 0 & 0 & 0 & 0 & 0 & 0 & 1 \cdots & 0 \end{bmatrix}$$
$$L_2 = \begin{bmatrix} L_{X_S} & L_{Y_S} & L_{Z_S} \end{bmatrix}^T$$

The least squares solution of unknown parameters is：

$$X = \left(A_1^T P_1 A_1 + A_2^T P_2 A_2\right)^{-1} \left(A_1^T P_1 L_1 + A_2^T P_2 L_2\right) \tag{14}$$

3.3 DEM Generation

Using the equation (11),we can calculate the three dimensional coordinates of each point in SAR image. Because of the array of unevenly spaced grid,the interpolation is needed. To obtain an evenly spaced grid, we use the bilinear interpolation method for simplicity without losing too much information.

4 TEST AREA AND RESULTS

Test area is Etna area in Italy. The interferometric SAR data were acquired by ERS-1/2 satellites. The area size is 30.7 km in azimuth and 40.9km in ground. The parameters of data are shown in table 1.

The processing results are shows in Fig.3—Fig.6. Fig.3 shows the intensity image of orbit 1,and has been processed for multi-look, 2 in range and 10 in azimuth(or 20 looks). The interferometric fringe is shown in Fig.4. Fig.5 shows the coherence map between two complex images, and average coherence is 0.56. Fig.6 is DEM image.

Table 1 Parameters of ERS-1/2 interferometric data in Etna ,Italy

Parameters	Orbit 1	Orbit 2
Satellite	ERS-1	ERS-2
Orbit number	21660	1987
Imaging time	1995.9.5	1995.9.6
Radar wavelength(m)	0.056	0.056
Azimuth pixel spacing(m)	3.9	3.9
Range pixel spacing(m)	7.9	7.9
Look number	1	1
Azimuth size(km)	30.720	30.720
Slant range size(km)	16.179	16.179
Ground range size(km)	40.96	40.96

In orde to translate the unwrapped phases into the elevations,we have to estimate the baseline,orbit and attitude parameters. The baseline vector is roughly estimated by using ERS-1/2 orbital data. We identified twelve ground control points from 1:50000 map and SAR image. Seven points are used to refine baseline and solve the orbit as well as attitude parameters,and other five points are used to check the accuracy.The rms of height check points is 11.3m. The three-dimensional coordinates for each point are calculated by using equation(11) and unwrapped phase.

5 CONCLUSIONS

We have developed a new software on PC's for interferometric SAR data processing. The least-squares matching is

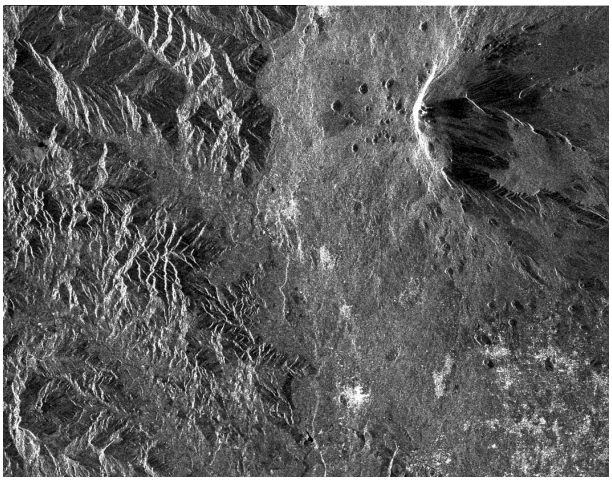

Fig.3 Intensity image relative to Mt.Etna

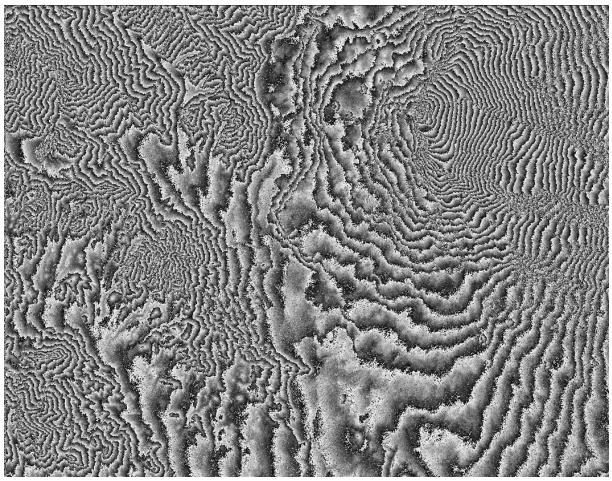

Fig.4 Flat terrain filtered fringe image

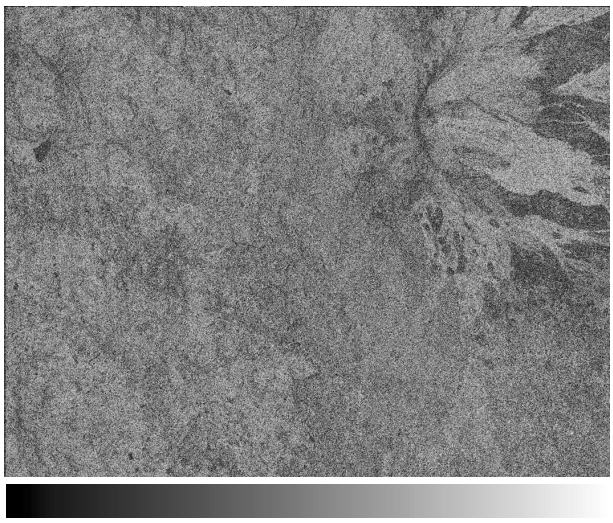

0 1(rad)

Fig. 5 Coherence image

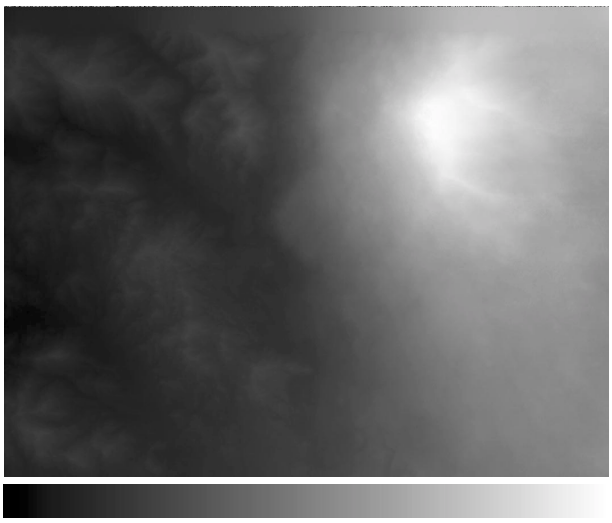

500 1000 1500 2000 2500 3000 3500(m)

Fig. 6 INSAR derived DEM

used to register the complex SAR pair. The accuracy of 0.03 pixel size is achieved. A new set of equations for calculating the three-dimensional coordinates of target point have also been presented. This equation more accurately describes the dynamitic imaging geometry of interferometric SAR. Using at least six ground control points. it is possible to refine interferomeric baseline, and estimate phase constant, the orbit and attitude parameters simultaneously. The processing results for ERS-1/2 interferometric SAR over the Etna in Italy verify our method. The rms for five ground height check points is 11.3m. We plan to compare INSAR DEM with reference DEM.

ACKNOWLEDGMENTS

I would like to thank D.Massonnet, French Space Agency(CNES) for providing the interferometric data in Etna area.

REFERENCES

Ghiglia,D.C. and Romero,L.A.,1994.Robust two-dimensional weighted and unweighted phase unwrapping that uses fast transforms and iterative methods. J.Opt.Soc.Am., 11,pp.107-117.

Goldstein,R.M.,Engelhardt,H., Kamb,B., and Frolich,R.M.,1993.Satellite radar interferometry for monitoring ice sheet motion: Application to an Antarctic ice stream. Science, 262, pp.1525-1530.

Goldstein,R.M.,Zebker,H.A., and Werner,C.,1988.Satellite radar interferometry: two-dimensional phase unwrapping. Radio Sci, 23,pp.713-720.

Massonnet,D. et al.,1993.The displacement field of the landers earthquake mapped by radar interferometry. Nature,364,pp.138-142.

Shuttle Radar Topography Mission(SRTM),http://www.nima.mil(1999)

Shi,S.P. and Chen,B.Y.,1996.Principle of interferometric SAR for topographic mapping and digital simulation. Journal of xi'an research institute of surveying and mapping(in Chinese),14,pp. 8-17.

Zebker,H.A. and Goldstein,R.M.,1986. Topographic mapping from interferometric SAR observations. J.Geophys.Res.,91(5),pp.4993-4999.